

Human Cytomegalovirus Directly Induces the Antiviral Protein Viperin to Enhance Infectivity

Jun-Young Seo, Rakina Yaneva, Ella R. Hinson, Peter Cresswell*

Viperin is an interferon-inducible protein that is directly induced in cells by human cytomegalovirus (HCMV) infection. Why HCMV would induce viperin, which has antiviral activity, is unknown. We show that HCMV-induced viperin disrupts cellular metabolism to enhance the infectious process. Viperin interaction with the viral protein vMIA resulted in viperin relocation from the endoplasmic reticulum to the mitochondria. There, viperin interacted with the mitochondrial trifunctional protein that mediates β -oxidation of fatty acids to generate adenosine triphosphate (ATP). This interaction with viperin, but not with a mutant lacking the viperin iron-sulfur cluster-binding motif, reduced cellular ATP generation, which resulted in actin cytoskeleton disruption and enhancement of infection. This function of viperin, which was previously attributed to vMIA, suggests that HCMV has coopted viperin to facilitate the infectious process.

The importance of the type 1 interferon (IFN) pathway in directing the antiviral response is well established (1, 2). Although many proteins are induced by IFN stimulation or viral infection (1, 2), the functions of most of them remain unexplored. Moreover, despite the antiviral effects of IFN-inducible proteins, some viruses directly induce them for reasons that are largely not well understood. Viperin is an IFN-inducible iron-sulfur (Fe-S) cluster-binding antiviral protein (3–5). It is induced in various cell types by both type I and

II IFNs, polyinosinic:polycytidylic acid, double-stranded RNA (dsRNA), viral DNA, and lipopolysaccharide and by infection with many viruses, including human cytomegalovirus (HCMV) (5–13). Although viperin inhibits HCMV infection when preexpressed in cells (5), the virus directly induces viperin expression independently of IFN production (13). This suggests that viperin induction might be advantageous to the virus.

As an initial approach to the potential mechanism, we investigated the intracellular distribu-

tion of viperin during HCMV infection (14). We previously showed that viperin is redistributed from the endoplasmic reticulum (ER) through the Golgi to the virus assembly compartment (AC) upon HCMV infection and suggested that this reflected a strategy to evade the antiviral effects of ER-localized viperin (5). Consistent with previous studies, IFN-induced viperin localized to the ER (fig. S1A). We were surprised, however, to observe that viperin induced in human foreskin fibroblasts (HFFs) by HCMV infection could be detected in association with mitochondria at 1 day post infection (dpi) (fig. S1B) and at the AC at 3 to 4 dpi (fig. S1C). The viral mitochondrial inhibitor of apoptosis (vMIA) is an HCMV-encoded protein known to traffic to mitochondria (15–18), which suggested a possible mechanism for mitochondrial targeting of viperin during HCMV infection. We observed that viperin colocalized with vMIA to the mitochondria at 1 dpi (Fig. 1A). At 3 dpi viperin was redistributed to the AC, although vMIA remained associated with the mitochondria (Fig. 1A). Coimmunoprecipitation experiments showed that endogenous viperin and vMIA can interact with each other in virally

Department of Immunobiology, Howard Hughes Medical Institute, Yale University School of Medicine, 300 Cedar Street, New Haven, CT 06520–8011, USA.

*To whom correspondence should be addressed. E-mail: peter.cresswell@yale.edu

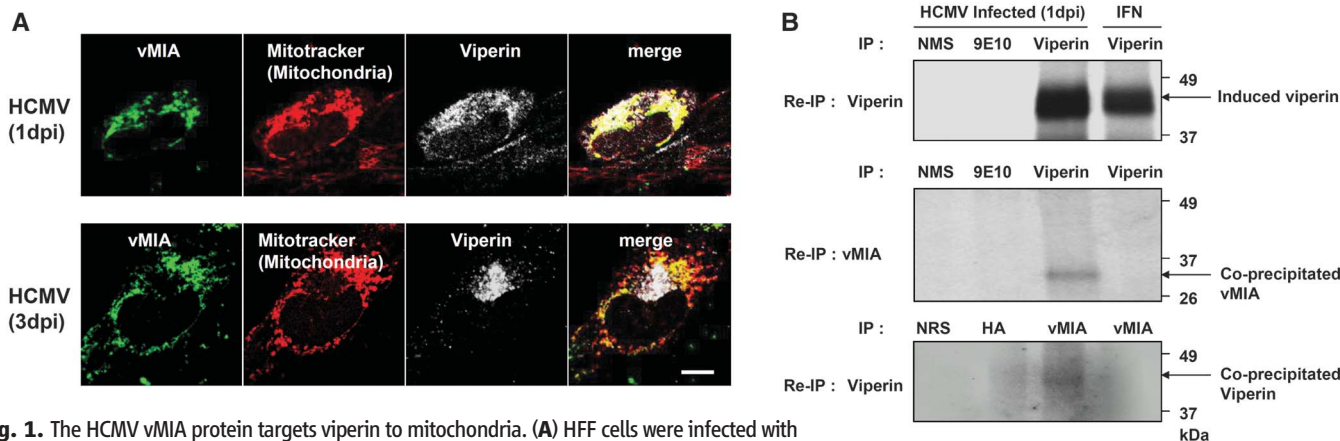


Fig. 1. The HCMV vMIA protein targets viperin to mitochondria. **(A)** HFF cells were infected with HCMV at a multiplicity of infection (MOI) of 2 for 1 or 3 days. Cells were stained with antibodies against vMIA (4B6-B) and viperin (MaP.VIP), and MitoTracker Red. A representative image from two individual experiments is shown. **(B)** HFF cells were infected with HCMV at a MOI of 2 for 1 day or treated with IFN- α (1000 U/ml) for 16 hours. Cells were labeled with [35 S]methionine-cysteine for 2 hours and lysed in detergent. The immunoprecipitation was performed with normal mouse serum (NMS), antibody against Myc (9E10), or MaP.VIP antibody (top and middle). The precipitates were SDS stripped, and released material was reimmunoprecipitated with MaP.VIP (top) or an antibody against vMIA (DC35) (middle). The reciprocal immunoprecipitation was performed with normal rabbit serum (NRS), hemagglutinin (HA)-specific antibody or DC35 antibody, and the stripped immunoprecipitates were reimmunoprecipitated with MaP.VIP (bottom). Coimmunoprecipitated vMIA or viperin were detected after SDS polyacrylamide gel electrophoresis (SDS-PAGE). **(C)** HFF cells transiently expressing viperin and/or vMIA-Myc were examined by immuno-EM. The sections were stained first with antibodies against viperin and/or Myc (9E10) and then with a secondary antibody, 5- or 10-nm gold conjugate, respectively. A representative field is shown (Nu, nucleus; Mito, mitochondria). The arrows indicate gold-labeled viperin and vMIA-Myc. A representative image from two individual experiments is shown. Scale bars, 10 μ m (A) and 200 nm (C).

infected cells (Fig. 1B). The viperin interaction with vMIA was confirmed in transiently expressing cells by cross-linking followed by solubilization and immunoprecipitation (fig. S2A) and by fluorescent protein-fragment complementation analysis (PCA) (fig. S2, B to E). Analysis by immunoelectron microscopy (immuno-EM) (Fig. 1C) or confocal immunofluorescence microscopy (fig. S2F) also confirmed that the vMIA interaction directly induced viperin targeting to mitochondria.

vMIA has been reported to be responsible for the disruption of the actin cytoskeleton observed after HCMV infection that is believed to facilitate infection (19–23). The vMIA-induced redistribution of viperin to mitochondria suggested that

this effect might be indirect. To examine this question, we used murine embryonic fibroblasts (MEFs) from viperin-depleted (knockout, KO) mice or COS-7 cells, in which endogenous viperin is not induced by double-stranded DNA transfection as it is with HFFs (fig. S3, A and B). The redistribution of viperin by vMIA was also seen in cotransfected MEFs (fig. S3C). We monitored alterations of the actin cytoskeleton in cells transiently expressing vMIA and/or viperin by staining with phalloidin (Fig. 2 and fig. S4). Consistent with previous reports (19, 20), cytoskeletal organization was markedly disrupted, with loss of stress fibers, in wild-type (WT) MEFs expressing vMIA alone, in which endogenous viperin is induced by the transfection protocol (Fig. 2A).

However, the actin cytoskeleton was indistinguishable from that of nontransfected cells when vMIA was expressed in viperin KO MEFs, where no endogenous viperin is induced (Fig. 2A). When viperin and vMIA were coexpressed in viperin KO MEFs, the actin cytoskeleton was dramatically disrupted (Fig. 2B). This suggests that viperin is required for the vMIA-induced disruption of the actin cytoskeleton. The actin cytoskeleton was maintained in all cell types expressing viperin alone (fig. S4A). The same patterns of cytoskeletal disruption were also observed in COS-7 cells (fig. S4B). We quantified the actin stress fibers by measuring the phalloidin intensity in three-dimensional images of cells transiently expressing vMIA and/or viperin (fig. S4C). In comparison

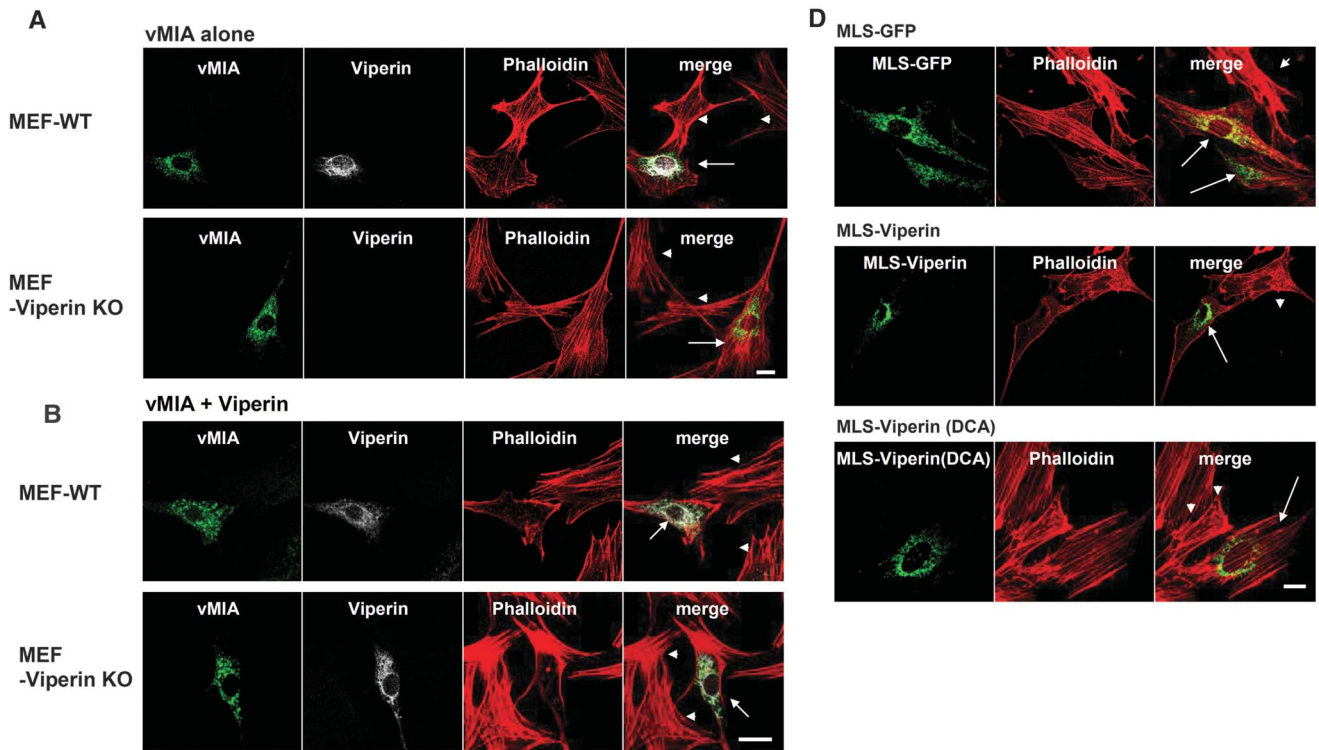


Fig. 2. Mitochondrial viperin is responsible for disrupting the actin cytoskeleton. (A and B) WT or viperin KO MEFs were transiently transfected with plasmids expressing vMIA and/or viperin. Cells were stained with antibodies against vMIA (4B6-B) and/or viperin (MaP.VIP), and Alexa Fluor 546 phalloidin was used to visualize F-actin. The arrows indicate transfected cells and the arrowheads, nontransfected cells. A representative image from three individual experiments is shown. (C) Actin stress fibers were quantified in MEFs expressing vMIA and/or viperin. The mean values from transfected cells were normalized to those (set as 100) from nontransfected cells on the same image. Data are presented as means of three independent experiments ($n = 6$ to 7) \pm SEM. * $P < 0.001$. (D) The N-terminal 42 residue α -helical region of viperin WT or viperin (DCA) was replaced by a mitochondrial localization sequence (MLS, amino acids 2 to 34) of vMIA. The MLS was directly fused to enhanced green fluorescent protein (EGFP) as a negative control. Viperin KO MEFs transiently expressing the indicated chimeric viperin proteins were stained with MaP.VIP

antibody and Alexa Fluor 546 phalloidin. The arrows indicate transfected cells and the arrowheads, nontransfected cells. A representative image from three individual experiments is shown. (E) Actin stress fibers were quantified as described above. Data are presented as means of three independent experiments ($n = 5$ to 8) \pm SEM. * $P < 0.001$. Scale bars, 20 μ m (A, B, and D).

with nontransfected cells, the phalloidin intensities in WT MEFs expressing vMIA alone, or both WT and viperin KO MEFs coexpressing viperin and vMIA, were reduced by about 50 to 60%, whereas the intensity in viperin KO MEFs expressing vMIA alone was not reduced (Fig. 2C). These results suggest that viperin targeting to mitochondria is required for the disruption of the actin cytoskeleton.

To identify viperin elements involved in the disruption of the actin cytoskeleton, two mutated constructs were used. In the first, residues 1 to 42 were deleted [viperin (Δ N)] to eliminate ER association (24), and in the second, two cysteine residues (88 and 91) were mutated to alanine to eliminate Fe-S cluster association [viperin (DCA)]. When viperin (Δ N) and vMIA or viperin (DCA) and vMIA were coexpressed in viperin KO MEFs, viperin (Δ N) was distributed throughout the cytoplasm, whereas viperin (DCA) colocalized with vMIA in mitochondria (fig. S5A). The lack of

vMIA interaction with viperin (Δ N) and the interaction of vMIA with viperin (DCA) were confirmed by PCA analysis (fig. S5, B and C). When we examined the cells coexpressing these proteins, however, we observed that the actin cytoskeleton was maintained (fig. S5, D and E). These data indicated a requirement for both mitochondrial localization and Fe-S cluster binding for the viperin-mediated effects.

To determine whether vMIA played any additional role in the process, we generated chimeric WT and Fe-S cluster-binding mutant viperin constructs in which the N-terminal amphipathic α helix, responsible for ER and lipid droplet association (24, 25), was replaced by the mitochondrial localization sequence (MLS) of vMIA (fig. S6, A to C). We also generated a fusion construct with the MLS linked to green fluorescent protein (GFP) directly. We then examined the status of the actin cytoskeleton in viperin KO MEFs or COS-7 cells expressing each chimeric

protein (Fig. 2, D and E, and fig. S6D). Although the actin cytoskeleton was maintained in cells expressing MLS-GFP, it was disrupted by 60 to 70% in cells expressing MLS-viperin, which indicated that directly targeted viperin mediates actin cytoskeleton disruption independently of vMIA. Similar results were produced in viperin KO MEFs expressing a chimeric viperin protein in which the N-terminal amphipathic α helix was replaced by the MLS of Tom70, a host cellular mitochondrial protein (fig. S7); this finding excluded the possibility that the MLS from vMIA was responsible for the effect. The actin cytoskeleton was maintained in cells expressing MLS-viperin (DCA), again showing that Fe-S cluster binding is necessary for cytoskeletal disruption (Fig. 2, D and E, and fig. S6D).

Previous studies have shown that the actin cytoskeleton is disrupted by both ATP depletion and ischemia (26–28) and possibly by vMIA-mediated inhibition of mitochondrial ATP generation (19). To determine whether the reduction of ATP generation is mediated by vMIA or by associated viperin, we measured intracellular ATP levels in viperin KO MEFs expressing vMIA-Myc, WT viperin, or viperin mutants (Fig. 3A). ATP levels were reduced only in cells expressing MLS-viperin, by ~50%, which indicates that mitochondrially targeted, Fe-S cluster-binding viperin is responsible for the decrease (Fig. 3A).

A proteomics analysis of viperin-interacting proteins suggested that the ATP reduction induced by targeting viperin to mitochondria could involve a viperin interaction with the β subunit of the mitochondrial trifunctional protein (TFP) (fig. S8A). TFP is a multienzyme complex, composed of four α subunits (HADHA) and four β subunits (HADHB), that catalyzes the last three steps of fatty acid β -oxidation, a major mechanism of cellular ATP production (29, 30). We confirmed the interaction of HADHB with viperin by co-immunoprecipitation and by chemical cross-linking followed by solubilization and immunoprecipitation (Fig. 3B and fig. S8, B and C).

To assess whether the viperin interaction with HADHB affects cellular bioenergetics, we measured fatty acid oxidation levels, ADP/ATP ratios, and the ratios of the reduced form of nicotinamide adenine dinucleotide/nicotinamide adenine dinucleotide (NADH/NAD^+) in transfected viperin KO MEFs (fig. S8, D to F). Palmitate oxidation was reduced by 30% (fig. S8D), ADP/ATP ratios increased by 100% (fig. S8E), and NADH/NAD^+ ratios reduced by 35% only in cells expressing MLS-viperin (fig. S8F). Thus, mitochondrial localization and Fe-S cluster binding both appear to be essential for metabolic disruption.

To confirm that viperin interaction with HADHB is responsible for the metabolic effects observed, we adopted a genetic approach, measuring cellular ATP levels in patient-derived TFP-deficient human fibroblasts transiently expressing vMIA-Myc, WT viperin, or viperin mutants, with or without GFP tags (Fig. 3, C and D). In WT HFF cells expressing vMIA-Myc (which induces

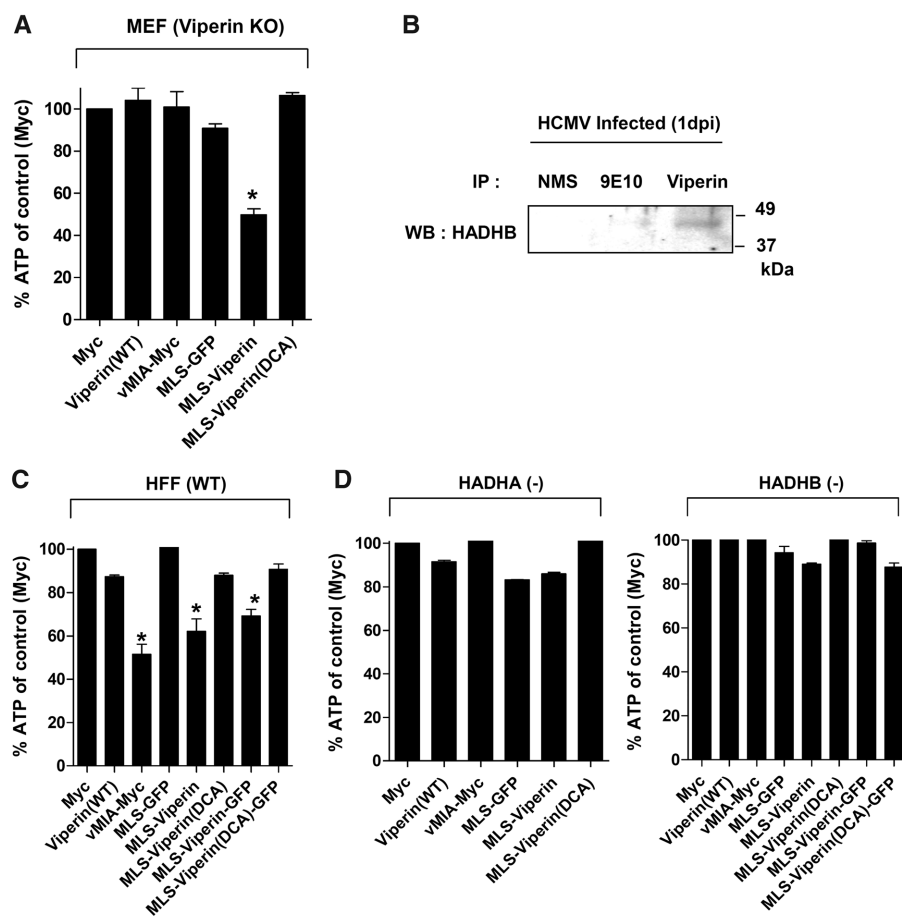


Fig. 3. Viperin interaction with mitochondrial TFP mediates reduction of cellular ATP levels. (A) Cellular ATP levels were measured in viperin KO MEFs transiently expressing the indicated proteins. The control value from Myc alone was set as 100%. Data are presented as means of three independent experiments \pm SEM. * $P < 0.001$. (B) Endogenous viperin interaction with the β subunit (HADHB) of TFP. HFF cells were infected with HCMV at a MOI of 2 for 1 day. Cells were lysed and immunoprecipitated with normal mouse serum (NMS) or antibodies against Myc (9E10) or viperin (MaP.VIP), and Western blots were probed using antibody against HADHB. (C and D) Cellular ATP levels were measured from WT (C) or TFP-deficient HFF cells [HADHA(-) or HADHB(-)] (D) transiently expressing the indicated proteins. Data are presented as means of at least two independent experiments \pm SEM. * $P < 0.001$.

endogenous viperin), MLS-viperin and MLS-viperin-GFP, the ATP levels were reduced to 50 to 70% of control levels (Fig. 3C). In HADHA-deficient or HADHB-deficient fibroblasts, however, ATP levels were unaffected (Fig. 3D), as was the actin cytoskeleton (fig. S8, G and H). Taken together, the data indicate that interaction of the mitochondrially targeted viperin with HADHB reduces TFP activity, which lowers cellular ATP levels and disrupts the actin cytoskeleton.

Finally, to assess whether viperin induced by HCMV infection also mediates actin cytoskeleton disruption, induction in HFFs [HFTelo cells expressing telomerase (31)] was suppressed by stably expressing two different short hairpin RNAs (shRNAs) (Fig. 4A). We then examined the actin cytoskeleton in viperin knockdown (KD) HFTelo cells after infection (Fig. 4A). In contrast to cells expressing no shRNA or control luciferase shRNA, in viperin KD cells the pattern of actin stress fibers was indistinguishable from that in non-infected cells (Fig. 4A), as were the ATP levels (Fig. 4B). We then asked if, as expected (21, 22), eliminating stress fiber disruption affected HCMV replication. We determined the kinetics of replication for viruses recovered from viperin KD cells by single-step growth assays. Although HCMV

production was unaffected at 3 days post infection, after 6 days it was reduced by more than 10-fold in the viperin KD cells compared with control shRNA-expressing cells (Fig. 4C). To exclude the possibility that viperin shRNA expression induced IFN- or dsRNA-dependent expression of other IFN-stimulated genes (ISGs) that might inhibit HCMV replication, we examined the expression of a variety of ISGs and found no induction (fig. S9, A and B). As a control for the specificity of the shRNA effects, we generated a recombinant HCMV (HCMV.mVIP) in which the loci US7-US16, nonessential for in vitro replication, were replaced by mouse viperin-GFP under an inducible promoter such that expression could be enhanced by the addition of doxycycline (fig. S9C). Expression of mouse viperin-GFP, not susceptible to the effects of the human-specific shRNAs, by HCMV.mVIP rescued the WT HCMV phenotype in viperin shRNA-expressing cells, both in terms of viral replication (Fig. 4D) and actin stress-fiber disruption (fig. S9D).

HCMV specifically targets viperin to mitochondria and uses its ability to inhibit TFP-mediated ATP generation to disrupt the actin cytoskeleton, which facilitates viral replication. These effects, previously attributed to vMIA, result from the

ability of vMIA to recruit induced endogenous viperin to mitochondria. Although mitochondrial viperin reduced ATP levels, it did not induce apoptosis in transiently transfected cells when we used terminal deoxynucleotidyl transferase-mediated deoxyuridine triphosphate nick end labeling (TUNEL) assays (fig. S10), which suggested that HCMV uses viperin to reduce ATP levels sufficiently to induce actin cytoskeleton disruption but not apoptosis. Although the precise mechanism by which viperin exerts its effect on TFP function remains unclear, immuno-EM showed that viperin and TFP are both detectable at the outer and inner mitochondrial membranes (fig. S11). Viperin interaction with TFP on the outer membrane may inhibit internalization and maturation of TFP, or viperin association with TFP on the inner membrane could directly inhibit its enzymatic activity.

We have observed a shift to glycolysis, which reduces the pH of the culture medium (fig. S12), when viperin is overexpressed in cells; this finding implies that TFP inhibition can occur with WT viperin. Presumably, this effect is exacerbated when viperin is driven to mitochondria by vMIA interaction or by providing it with an MLS. Cells may normally regulate a viperin mitochondrial function that is exploited by HCMV to inhibit

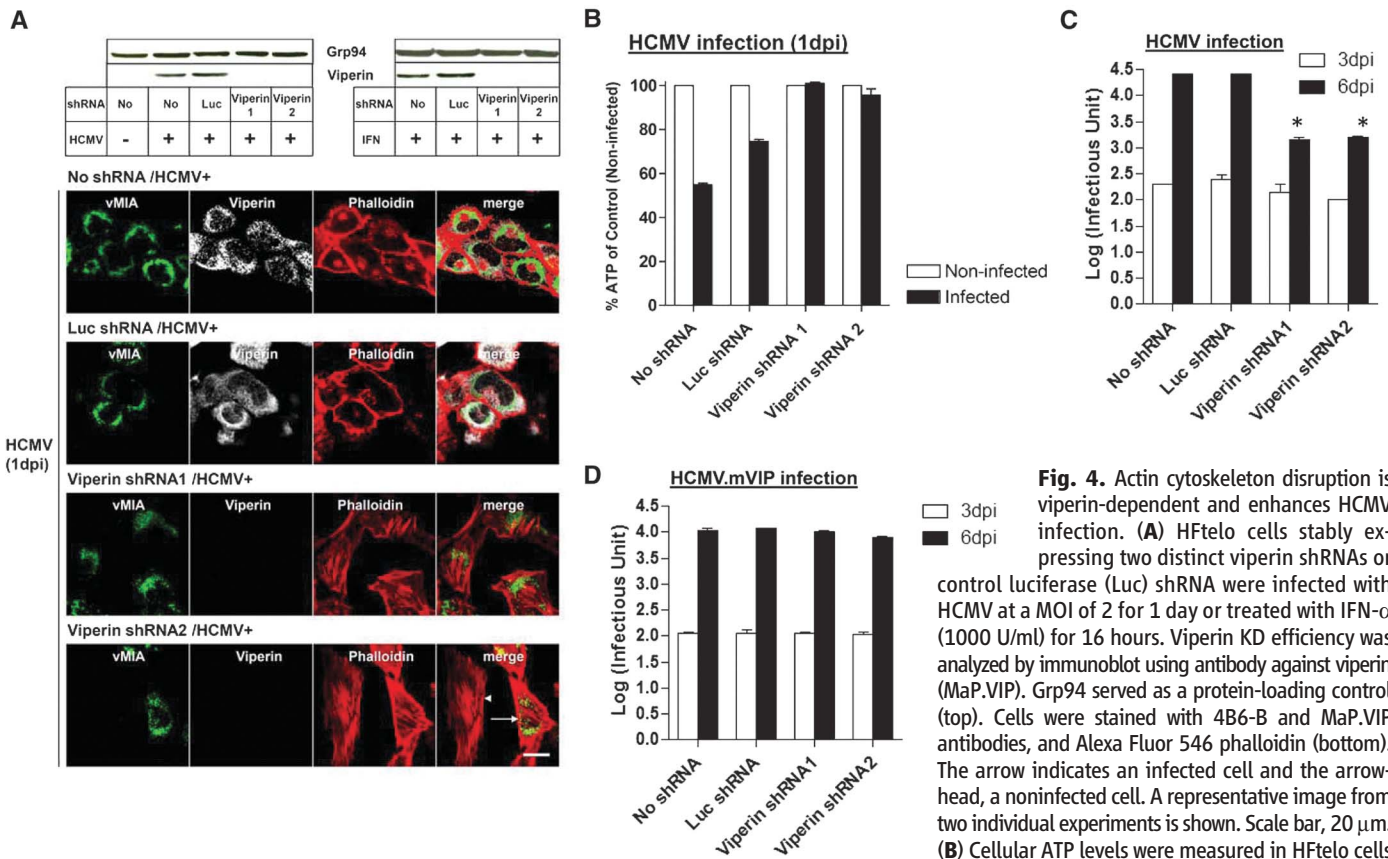


Fig. 4. Actin cytoskeleton disruption is viperin-dependent and enhances HCMV infection. (A) HFTelo cells stably expressing two distinct viperin shRNAs or control luciferase (Luc) shRNA were infected with HCMV at a MOI of 2 for 1 day or treated with IFN- α (1000 U/ml) for 16 hours. Viperin KD efficiency was analyzed by immunoblot using antibody against viperin (MaP.VIP). Grp94 served as a protein-loading control (top). Cells were stained with 4B6-B and MaP.VIP antibodies, and Alexa Fluor 546 phalloidin (bottom). The arrow indicates an infected cell and the arrowhead, a noninfected cell. A representative image from two individual experiments is shown. Scale bar, 20 μ m. (B) Cellular ATP levels were measured in HFTelo cells stably expressing the indicated shRNAs after infection with HCMV at a MOI of 2 for 1 day. The control (uninfected) was set as 100%. Data are presented as means \pm SEM of duplicate samples and are representative of two individual experiments. (C and D) HFTelo cells stably expressing the indicated shRNAs were infected with HCMV (C) or recombinant HCMV.mVIP, in which the loci US7 to US16 were replaced by doxycycline (Dox)-inducible mouse viperin-GFP (D), at an MOI of 0.2, and supernatants were harvested 3 or 6 dpi. Dox (2 μ g/ml) was added on day 0 and 3 (D). Virus yield was quantified by a fluorescence-based virus infectivity assay. Data are presented as means \pm SEM of duplicate samples and are representative of two individual experiments. * $P < 0.001$.

TFP-mediated ATP generation and to facilitate viral replication.

References and Notes

1. A. G. Bowie, L. Unterholzner, *Nat. Rev. Immunol.* **8**, 911 (2008).
2. A. J. Sadler, B. R. Williams, *Nat. Rev. Immunol.* **8**, 559 (2008).
3. K. S. Duschene, J. B. Broderick, *FEBS Lett.* **584**, 1263 (2010).
4. G. Shaveta, J. Shi, V. T. Chow, J. Song, *Biochem. Biophys. Res. Commun.* **391**, 1390 (2010).
5. K. C. Chin, P. Cresswell, *Proc. Natl. Acad. Sci. U.S.A.* **98**, 15125 (2001).
6. M. A. Rivieccio *et al.*, *J. Immunol.* **177**, 4735 (2006).
7. K. J. Ishii *et al.*, *Nat. Immunol.* **7**, 40 (2006).
8. M. Severa, E. M. Coccia, K. A. Fitzgerald, *J. Biol. Chem.* **281**, 26188 (2006).
9. H. S. Suh *et al.*, *J. Virol.* **81**, 9838 (2007).
10. P. Boudinot *et al.*, *J. Gen. Virol.* **81**, 2675 (2000).
11. J. Fink *et al.*, *PLoS Negl. Trop. Dis.* **1**, e86 (2007).
12. D. Jiang *et al.*, *J. Virol.* **82**, 1665 (2008).
13. H. Zhu, J. P. Cong, T. Shenk, *Proc. Natl. Acad. Sci. U.S.A.* **94**, 13985 (1997).
14. Materials and methods are available as supporting material on Science Online.
15. V. S. Goldmacher *et al.*, *Proc. Natl. Acad. Sci. U.S.A.* **96**, 12536 (1999).
16. V. S. Goldmacher, *Biochimie* **84**, 177 (2002).
17. H. O. Al-Barazi, A. M. Colberg-Poley, *J. Virol.* **70**, 7198 (1996).
18. A. M. Colberg-Poley, M. B. Patel, D. P. Erez, J. E. Slater, *J. Gen. Virol.* **81**, 1779 (2000).
19. D. Poncet *et al.*, *J. Cell Biol.* **174**, 985 (2006).
20. R. Sharon-Friling, J. Goodhouse, A. M. Colberg-Poley, T. Shenk, *Proc. Natl. Acad. Sci. U.S.A.* **103**, 19117 (2006).
21. N. L. Jones, J. C. Lewis, B. A. Kilpatrick, *Eur. J. Cell Biol.* **41**, 304 (1986).
22. S. Cudmore, I. Reckmann, M. Way, *Trends Microbiol.* **5**, 142 (1997).
23. X. Wang, D. Y. Huang, S. M. Huang, E. S. Huang, *Nat. Med.* **11**, 515 (2005).
24. E. R. Hinson, P. Cresswell, *J. Biol. Chem.* **284**, 4705 (2009).
25. E. R. Hinson, P. Cresswell, *Proc. Natl. Acad. Sci. U.S.A.* **106**, 20452 (2009).
26. E. A. Shelden, J. M. Weinberg, D. R. Sorenson, C. A. Edwards, F. M. Pollock, *J. Am. Soc. Nephrol.* **13**, 2667 (2002).
27. R. Bacallao, A. Garfinkel, S. Monke, G. Zampighi, L. J. Mandel, *J. Cell Sci.* **107**, 3301 (1994).
28. N. Golenhofen, R. B. Doctor, R. Bacallao, L. J. Mandel, *Kidney Int.* **48**, 1837 (1995).
29. K. Bartlett, S. Eaton, *Eur. J. Biochem.* **271**, 462 (2004).
30. S. Eaton *et al.*, *Biochem. Soc. Trans.* **28**, 177 (2000).
31. W. A. Bresnahan, G. E. Hultman, T. Shenk, *J. Virol.* **74**, 10816 (2000).

Acknowledgments: We thank C. Rahner in the Yale Center for Cell and Molecular Imaging for EM and the Keck Biotechnology Resource Laboratory for protein identification. The work was supported by the Howard Hughes Medical Institute. J.-Y.S. and P.C. conceived the study and designed experiments. J.-Y.S. performed experiments. R.Y. and E.R.H. performed assays and produced reagents. J.-Y.S. and P.C. analyzed and interpreted the data, and wrote the manuscript. All authors contributed to the final version of the manuscript.

Supporting Online Material

www.sciencemag.org/cgi/content/full/science.1202007/DC1
Materials and Methods
Figs. S1 to S12
References

21 December 2010; accepted 12 April 2011

Published online 28 April 2011;

10.1126/science.1202007

Deciphering the Rhizosphere Microbiome for Disease-Suppressive Bacteria

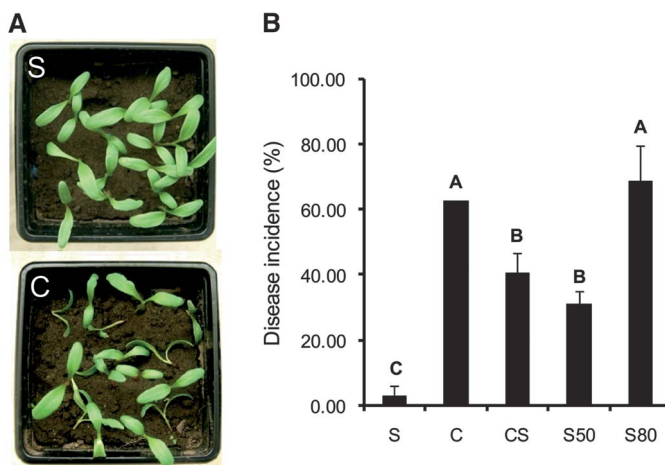
Rodrigo Mendes,^{1*} Marco Kruijt,^{1*} Irene de Bruijn,^{1§} Ester Dekkers,¹ Menno van der Voort,¹ Johannes H. M. Schneider,² Yvette M. Piceno,³ Todd Z. DeSantis,^{3,4} Gary L. Andersen,³ Peter A. H. M. Bakker,⁵ Jos M. Raaijmakers^{1¶}

Disease-suppressive soils are exceptional ecosystems in which crop plants suffer less from specific soil-borne pathogens than expected owing to the activities of other soil microorganisms. For most disease-suppressive soils, the microbes and mechanisms involved in pathogen control are unknown. By coupling PhyloChip-based metagenomics of the rhizosphere microbiome with culture-dependent functional analyses, we identified key bacterial taxa and genes involved in suppression of a fungal root pathogen. More than 33,000 bacterial and archaeal species were detected, with Proteobacteria, Firmicutes, and Actinobacteria consistently associated with disease suppression. Members of the γ -Proteobacteria were shown to have disease-suppressive activity governed by nonribosomal peptide synthetases. Our data indicate that upon attack by a fungal root pathogen, plants can exploit microbial consortia from soil for protection against infections.

Similar to other eukaryotes, plants and their microbiomes can be viewed as “super-organisms” in which the plant relies, in part, on the soil microbiota for specific functions and traits. In return, plants exude up to 21% of their photosynthetically fixed carbon in the root-

soil interface (1), i.e., the rhizosphere, thereby feeding the microbial communities and influencing their activity and diversity. For decades,

Fig. 1. (A) Effect of *R. solani* infection on growth of sugar beet seedlings in disease-suppressive (S) and disease-conducive (C) soils. **(B)** Percentage (mean \pm SEM, $N = 4$) of seedlings with damping-off symptoms in suppressive soil (S), conducive soil (C), conducive soil amended with 10% (w/w) of suppressive soil (CS), or suppressive soil heat-treated at 50°C (S50) or 80°C (S80). Different letters above the bars indicate statistically significant differences ($P < 0.05$, Student-Newman-Keuls).



¹Laboratory of Phytopathology, Wageningen University, Droevendaalsesteeg 1, Wageningen 6700 EE, Netherlands.

²Institute of Sugar Beet Research, Van Konijnenburgweg 24, Bergen op Zoom 4611 HL, Netherlands. ³Ecology Department, Lawrence Berkeley National Lab, Cyclotron Road 1, Berkeley, CA 94720, USA. ⁴Second Genome, Inc., Owens Street 1700, San Francisco, CA 94158, USA. ⁵Plant-Microbe Interactions, Department of Biology, Utrecht University, Padualaan 8, Utrecht 3584 CH, Netherlands.

*These authors contributed equally to this work.

†Present address: Brazilian Agricultural Research Corporation, Embrapa Environment, Jaguariuna, Brazil.

‡Present address: Monsanto Holland, Bergschenhoek, Netherlands.

§Present address: Institute of Medical Sciences, Aberdeen, Scotland, UK.

¶To whom correspondence should be addressed. E-mail: jos.raaijmakers@wur.nl



Human Cytomegalovirus Directly Induces the Antiviral Protein Viperin to Enhance Infectivity

Jun-Young Seo, Rakina Yaneva, Ella R. Hinson and Peter Cresswell (April 28, 2011)

Science **332** (6033), 1093-1097. [doi: 10.1126/science.1202007] originally published online April 28, 2011

Editor's Summary

This copy is for your personal, non-commercial use only.

- Article Tools** Visit the online version of this article to access the personalization and article tools:
<http://science.sciencemag.org/content/332/6033/1093>
- Permissions** Obtain information about reproducing this article:
<http://www.sciencemag.org/about/permissions.dtl>

Science (print ISSN 0036-8075; online ISSN 1095-9203) is published weekly, except the last week in December, by the American Association for the Advancement of Science, 1200 New York Avenue NW, Washington, DC 20005. Copyright 2016 by the American Association for the Advancement of Science; all rights reserved. The title *Science* is a registered trademark of AAAS.